DOI: 10.52846/AUCEE.2023.11

Modelling, Simulation and Implementation on dSpace 1103 of the Direct Power Control in a Three-Phase Shunt Active Power Filter System

Mihaiţă-Daniel Constantinescu, Mihaela Popescu, Gheorghe-Eugen Subţirelu and Ionuţ-Cosmin Toma
University of Craiova, Faculty of Electrical Engineering
mconstantinescu@em.ucv.ro, mpopescu@em.ucv.ro, esubtirelu@em.ucv.ro, ctoma@em.ucv.ro

***Abstract*— This article describes a control method called "direct power control" designed specifically for parallel active power filters. The purpose of this method is to attenuate harmonics in the supply current and offset reactive power problems. The main goal is to bring the active power and reactive power back to the reference values through hysteresis control. The output of the hysteresis controller is combined with the switching table to regulate active and reactive power in real time by determining the optimal switching configuration of the inverter. This study proposes a novel switching table design based on analyzing the impact of the inverter switching vector on the instantaneous reactive and active power derivatives. The goal is to reduce the number of commutations by eliminating zero vectors while maintaining the required DC bus voltage using anti-windup techniques based on PI controllers.**

Cuvinte cheie: *controlul direct al puterii(DPC), filtru activ, filtru activ de putere, putere reactivă.*

Keywords: *Direct Power Control (DPC), power quality, active power filter, active power, reactive power, switching table*

I. INTRODUCTION

Having the primary objective of enhancing the power quality of power sources and achieving unity power factor, the Voltage Source Inverters (VSIs) continue to play a significant role in various grid-connected applications. These applications encompass active power filters, and distributed generation systems utilizing renewable energy sources such as wind and photovoltaic power [1], [2].

The widespread adoption of static converters in both industrial and household devices, along with the use on an increasingly large scale of non-linear loads, has led to a significant power quality degradation especially through the current waveforms. This deterioration adversely impacts the reliability of power electronic equipment. Active power filters, with their diverse series, shunt, and hybrid configurations, have emerged as an appealing substitute for passive filters due to their advantages [1]. Usually, a three-phase Shunt Active Power Filter (SAPF), which employs a three-phase VSI is connected in parallel with the mains and non-linear loads at the Point of Common Coupling (PCC). The SAPF's purpose is to reduce current harmonics as much as possible, compensate reactive power, and maintain system stability. The effectiveness of SAPF relies on its power structure design, adopted control strategies, and the resilience of its controllers. Different control methods, such as some based on instantaneous reactive power theory and voltage-oriented control (VOC), have been explored to ensure optimal SAPF operation under varying conditions [1], [3]–[5].

Over the past decade, the Direct Power Control (DPC) method and others derived from it, such as Virtual Flux-DPC and DPC-Space Vector Modulation, were applied for PWM rectifiers and SAPFs [6]–[17]. Some of these applications have directly utilized Noguchi's switching table for DPC [6]. For the improvement of SAPF performance, the authors of [7] proposed an algorithm to compensate the harmonic current, redefined the switching functions, and dynamically adjusted the hysteresis bandwidths of the comparators. Different switching lookup tables for DPC used in an AC-DC converter were analyzed in [8].

In [9], a direct power control strategy for SAPF was presented, including experimental validation to illustrate the good dynamics of the system. Appropriate dynamic response of the supply current and DC voltage is also illustrated in [10].

The use of the direct power control in different applications, such as rectifiers, grid connected inverters and SAPF is well reviewed in [11].

Some new or improved switching tables to be used in DPC implementation are discussed in [12]–[16]. Also, the solution of using multiple switching tables for DPC is addressed in [17] and [18].

In the case of operation under non-ideal grid conditions, replacing the classical static look-up tables with the predictive DPC for the selection of the switching vector is proposed in [19].

In order to regulate DC-link voltage, a new control method using an anti-windup fractional order proportional-integral differentiator (AW-FOPID) controller is the solution proposed in [20]. A short response time in the DC-link voltage evolution, as well as small overshoots and undershoots are highlighted.

To compensate the harmonic currents in a grid-connected photovoltaic system, the hysteresis control and the DPC are the two methods analyzed comparatively in [21]. The superior performances related to the DPC method are highlighted.

Aiming to reduce the instantaneous active and reactive power ripples when conventional DPC is used, the replacement of the hysteresis controllers and switching table by a fuzzy inference system is proposed in [22]. In this way, a smother control is obtained.

This paper is focused on the implementation of the Direct Power Control algorithm in the control of a three-

phase SAPF system for the compensation of the current harmonics and reactive power. First, the system is described through its configuration, the calculation of the instantaneous powers, the hysteresis controllers and the switching table. Then, modelling, simulation and implementation of the system operation are presented in section III. For the experimental implementation of the control strategy, the dSPACE DS1103 PPC Controller Board woring with MATLAB-SIMULINK RTW was used and some experimental results are presented in section IV. At the end of the work, some final conclusions are drawn.

II. System Description

A. System Configuration

The power configuration of the SAPF system based on DPC is shown in Fig. 1. The ultimate goal is to compensate both the current harmonics and the reactive power so that the power factor at the supply side to be as close as possible to one.

The active power filter can operate as a controlled current source and it is required to deliver a supply current waveform that closely aligns with the reference current.

To establish the reference current, it is necessary to establish a balance between the instantaneous power provided by the source and the active power filter, and the load power. If notations p_s and q_s are used for the real instantaneous power and imaginary instantaneous power respectively at the supply side, for the purpose of offsetting the reactive power and eradicating harmonic currents, these powers should be $p_s = \bar{p}_l$ and $q_s = 0$ after compensation. p_l is the instantaneous power of the load and $\bar{p}_l$ is its average value.

If p_f and q_f denote the real and imaginary instantaneous power provided by SAPF and q_l is the instantaneous reactive power of the load, the following relationships can be expressed.

$$p_s = \bar{p}_l;\ q_s = 0; \tag{1}$$

$$p_f = p_l - p_s = \bar{p}_l + \tilde{p}_l - p_s = \bar{p}_l + \tilde{p}_l - \bar{p}_l = \tilde{p}_l \tag{2}$$

$$q_f = q_l - q_s = q_l \tag{3}$$

The oscillatory component of p_l should be supplied by the active power filter, whereas q_l must be entirely sourced from the active power filter. This approach enables the attainment of power compensation as well.

B. Instantaneous Powers Calculation

Based on the supply voltages and currents, the instantaneous active and reactive powers can be computed as the real and imaginary parts of the instantaneous apparent power or by using directly the measured quantities, as follows [6]:

$$p = e_a i_a + e_b i_b + e_c i_c \tag{4}$$

$$q = \frac{1}{\sqrt{3}}\left[(e_a - e_b)i_c + (e_b - e_c)i_a + (e_c - e_a)i_b\right] \tag{5}$$

In order to increase the system reliability by reducing the number of the used sensors, Noguchi formulated the so called sensorless DPC which is based on the estimated voltage in the point of common coupling [16], [22].

However, it should be noted that, in this approach, the time derivatives of the measured currents are used and the effect can be the increase of the harmonic distortion of the current [16].

C. Hysteresis Controllers

As shown in Fig. 1, two hysteresis band controllers are used in order to keep the instantaneous active and reactive powers into a desired band. Their inputs are the power errors, respectively the differences between the reference and calculated values of the active and reactive powers:

$$\begin{cases} \Delta p = P_{ref} - p \\ \Delta q = Q_{ref} - q \end{cases} \tag{6}$$

As illustrated in Fig. 2, the outputs of the hysteresis band controllers depend on the input errors (Δp and Δq) and the imposed hysteresis band for the active and reactive powers (HB(p, q)). The following expressions summarize the behavior of the hysteresis controller with respect to power error limits [16]:

$$\begin{aligned} &\Delta(p,q) > HB(p,q) \\ &-HB(p,q) \le \Delta(p,q) \le HB(p,q) \\ &\frac{d(\Delta(p,q))}{dt} < 0; \quad \Delta(p,q) = 1 \end{aligned} \tag{7}$$

$$\begin{aligned} &\Delta(p,q) < HB(p,q) \\ &-HB(p,q) \le \Delta(p,q) \le HB(p,q) \\ &\frac{d(\Delta(p,q))}{dt} > 0; \quad \Delta(p,q) = 0 \end{aligned} \tag{8}$$

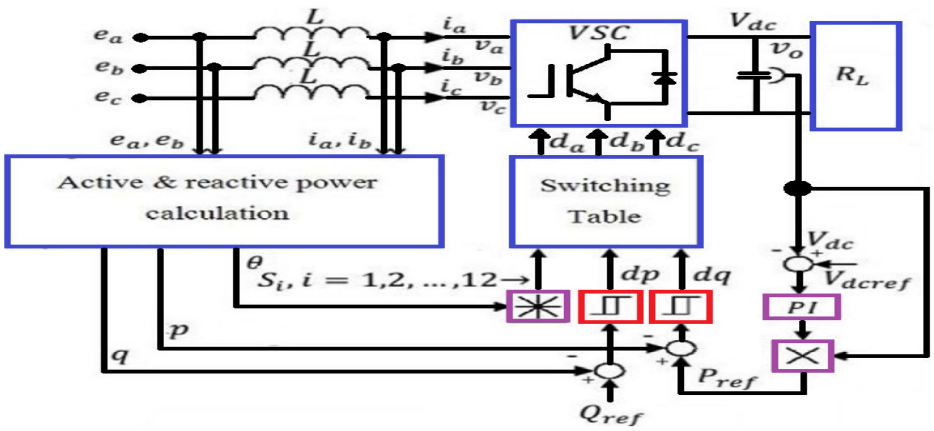

Fig. 1. Configuration of SAPF system based on DPC.

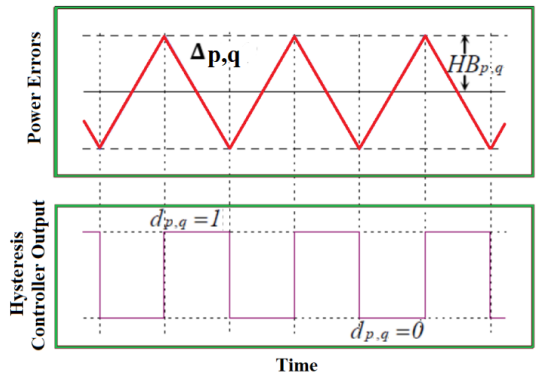

Fig. 2. Behavior of the hysteresis power comparator.

These outputs of the hysteresis controllers, together with the identified sector number of the voltage vector are the inputs of the switching table which will determine the appropriate switching of the inverter.

D. Swiching Table

The look-up table, commonly referred to as the switching table (ST) is a crucial component in the DPC technique. It was initially used in publications relating to the Direct Torque Control (DTC) of the induction motor [23].

ST plays an essential role in selecting the states of the VSI's power semiconductor devices to efficiently regulate the active and reactive powers. This component is used to determine how the transistors in the VSI are activated and deactivated to achieve the desired power values.

Using a switching table in direct power control offers advantages such as simplifying control, eliminating internal current control loops and PWM modulators, which can lead to a more efficient and faster implementation of the control technique.

In the context of DPC, in order to regulate the active and reactive powers to their reference values, quick and precise decisions need to be made regarding the switching states of the semiconductor devices in the VSI. This is where the switching table comes into play, providing clear instructions on how transistors or IGBTs should be turned on or off at each moment to fulfill the control objectives.

Usually, the switching table is prepared in advance and contains all possible switching combinations, each with its role in adjusting the active and reactive powers. It can be created based on certain criteria, such as errors related to the active and reactive powers or the position of the voltage vector.

Using these criteria, the DPC control decides which switching combinations to activate in order to achieve the desired regulation.

The primary goal when designing an ST is to ensure the accurate tracking of the two instantaneous powers. However, certain degrees of flexibility are present when pursuing this objective, affording the designer the option to alternatively emphasize dynamic properties or system efficiency [17].

Furthermore, the operational mode of the converter (either rectifier or inverter) or the grid sequence (positive or negative) should also be factored into the design process due to the impracticality of developing a single ST capable of delivering optimal performance across all these scenarios.

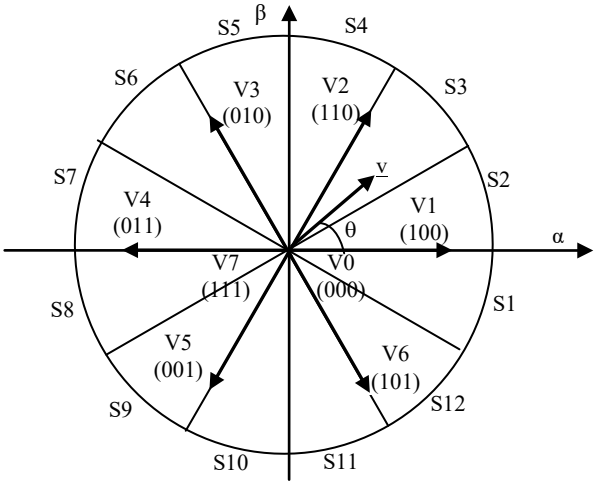

Fig. 3. Sectors and voltage vectors in the stationary reference frame.

To conceive the ST, the stationary reference frame α–β is divided into 12 sectors (Fig. 3). The number of the sector where the voltage vector is located can be simply determined by using same comparators [24].

The DC voltage control block gives the prescribed active power and the prescribed reactive power is an external quantity.

The hysteresis controllers outputs are the digitized signals dp and dq. Based on dp, dq and the number of the sector located for the voltage vector, the ST detailed in Table I gives the control signals of the converter's transistors [6], [8].

III. Modelling, Simulation and Implementation of the System Operation

The simulation of the SAPF system operation is based on the specific model conceived for the whole system in the MATLAB - SIMULINK environment (Fig. 4). It consists of several dedicated blocks for: the three-phase power supply, the non linear load which is an uncontrolled rectifier with RLC load, the PWM VSI, the control algorithm implementing the direct power control.

Fig. 5 illustrates the structure of the block named "Algorithm Control", according to the direct power control principles.

To highlight the correct operation of the control system, the waveforms of the phase voltage and supply current after compensation are illustrated Fig. 6. It must be specified that the supply current (in red in Fig. 6) is multiplied by 2 for qualitative identification. It can be seen that the compensated supply current is almost sinusoidal. For comparison, Fig. 7 shows the waveforms of the phase voltage and the high distorted load current.

TABLE I. Switching Table for the Adopted DPC

dp	dq	θ_1	θ_2	θ_3	θ_4	θ_5	θ_6	θ_7	θ_8	θ_9	θ_{10}	θ_{11}	θ_{12}
1	0	101	111	100	000	110	111	010	000	011	111	001	000
	1	111	111	000	000	111	111	000	000	111	111	000	000
0	0	101	100	100	110	110	010	010	011	011	001	001	101
	1	100	110	110	010	010	011	011	001	011	101	101	100

.

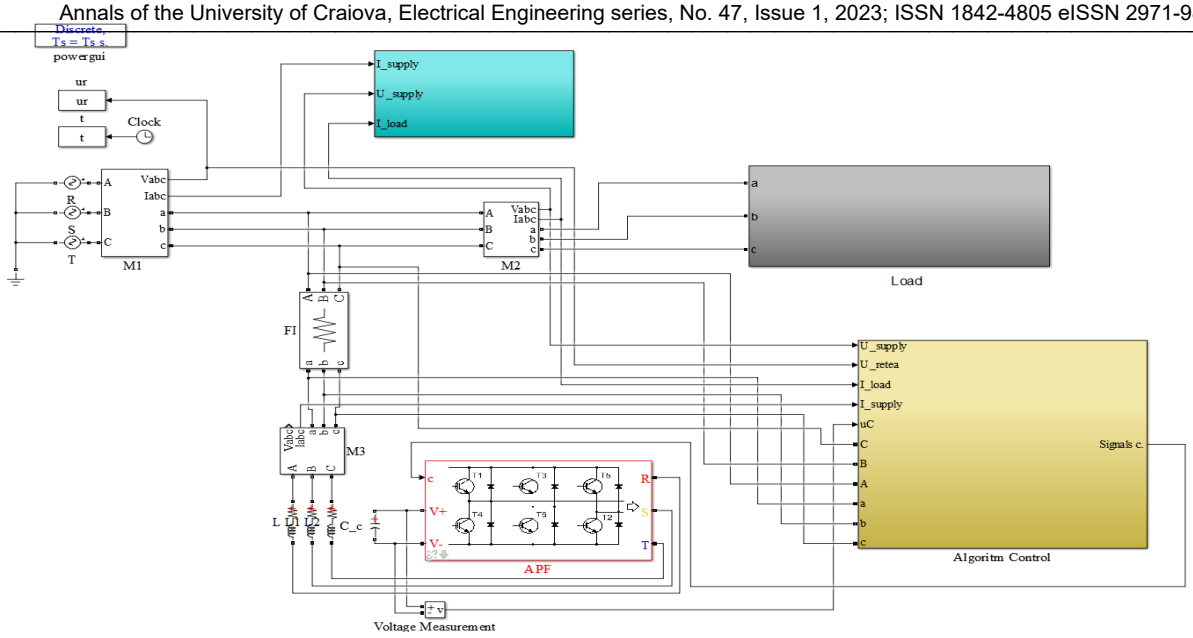

Fig. 4. The Matlab Simulink model of the SAPF compensation system with DPC.

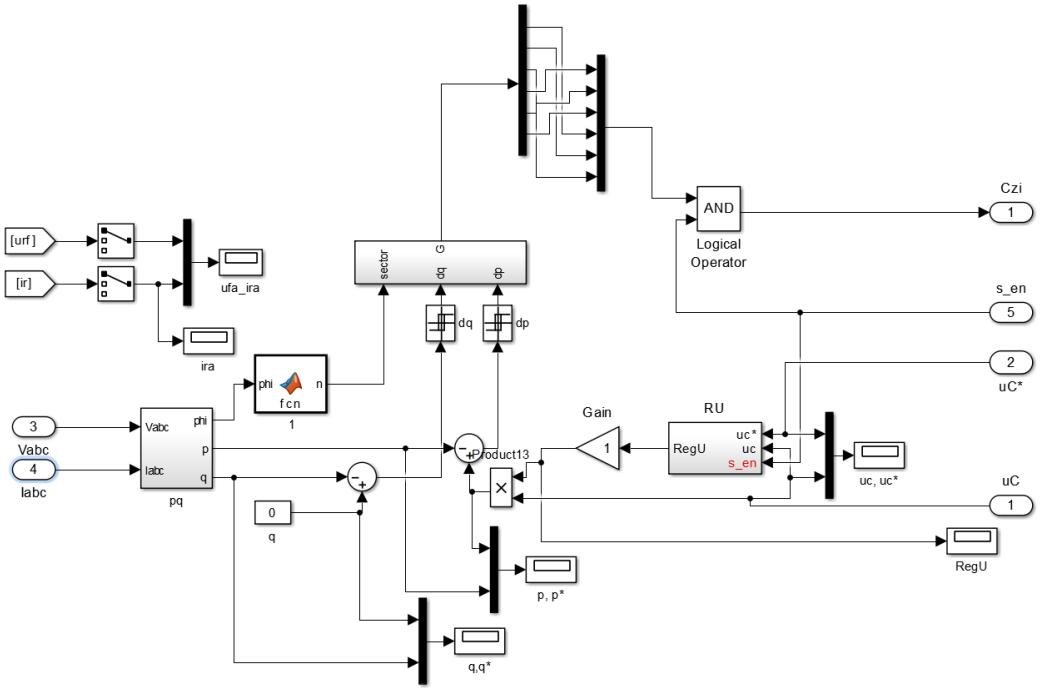

Fig. 5. The structure of the DPC block.

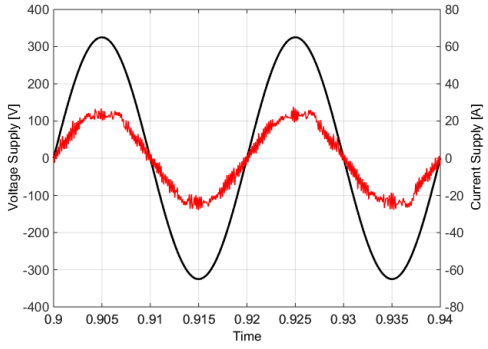

Fig. 6. Waveforms of the phase voltage and supply current, after compensation.

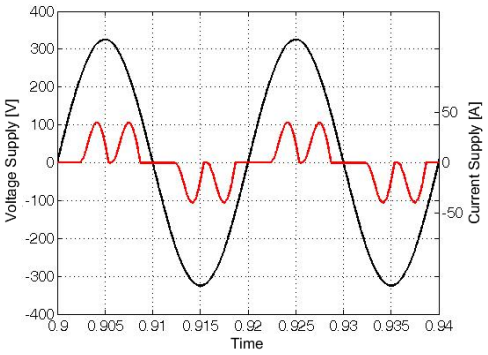

Fig. 7. Waveforms of the phase voltage and distorted load current.

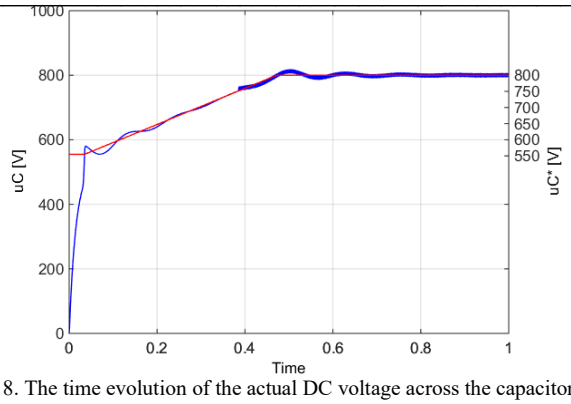

Fig. 8. The time evolution of the actual DC voltage across the capacitor (in blue) and its prescribed voltage (in red).

To illustrate the correct operation of the DC-voltage control loop, the actual voltage across the capacitor (in blue) and its prescribed value (in red) are shown in Fig. 8. It can be seen the faithful tracking of the prescribed value and that there is practically no steady state error, compared to the imposed value of 780 V.

IV. Experimental Verification

The experimental verification was done on a test bench for the SAPF system within the Research Centre for Electrical Engineering of the University of Craiova.

The control strategy is executed through a single-board dSPACE DS1103 PPC Controller Board, with integrated development environment of MATLAB-SIMULINK RTW, provided by MathWorks, Inc. The adopted sampling time used in the experimental tests is 25 μs, and experimental results are derived using identical parameters as those used in the simulation.

A picture of the conceived user interface by using Control Desk 5.3 is shown in Fig. 9. Both experimental results and the control panel are illustrated, as follows. The supply phase voltage and current after compensation are shown in the top left figure. It can be seen that they are in phase and the current is very close to the sinusoidal form, so the active filtering results are very good. The total harmonic distortion (THD) factor of the compensated current is about 7.2 %. Below these waveforms, the phase supply phase voltage and the distorted load current are displayed. In the bottom left figure, the three phase currents at the supply side after compensation are shown proving the balanced operation. In the upper-right corner, the control options for the algorithm are displayed, followed by the DC capacitor voltage (prescribed and actual values) waveforms.

An additional analysis was performed using a Fluke 41B harmonic analyzer for same measurements and experimental acquisitions. The results shown in Fig. 10 – Fig. 15 correspond to a load current of about 10 A. Thus: the acquired supply current after compensation is shown in Fig. 10; its harmonics spectrum is shown in Fig. 11; the numerical values associated with this current are shown in Fig. 12. With reference to the supply voltage, Fig. 13 illustrates its waveform, Fig. 14 its harmonics spectrum and Fig. 15 the associated numerical values.

It must be specified that the supply voltage available in the experiments has a small harmonic distortion of about 1.8 %.

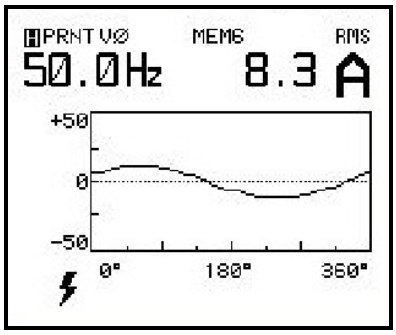

Fig. 10. Acquired supply current after compensation.

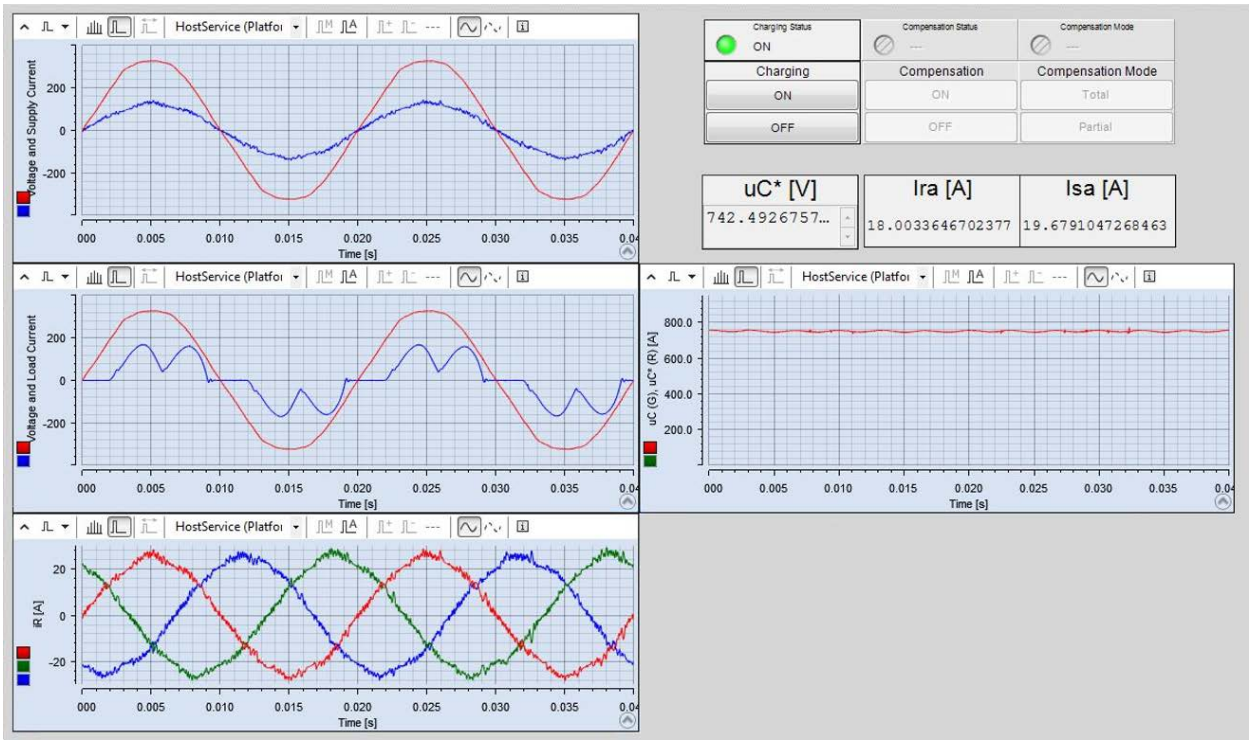

Fig. 9. The dSPACE Control Desk user interface.

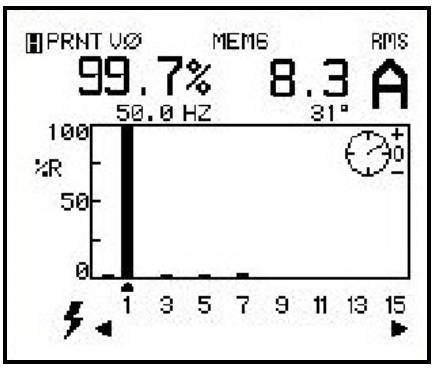

Fig. 11. Harmonics spectrum of the supply current after compensation.

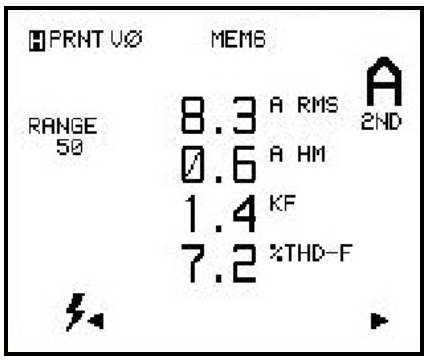

Fig. 12. The screen with the numerical values related to the supply current after compensation.

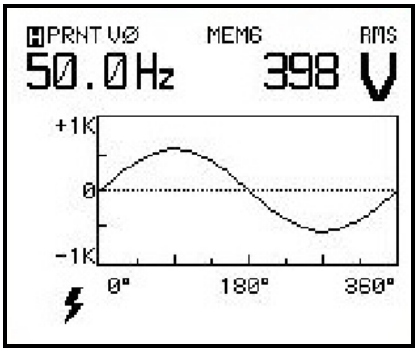

Fig. 13. Acquired supply voltage.

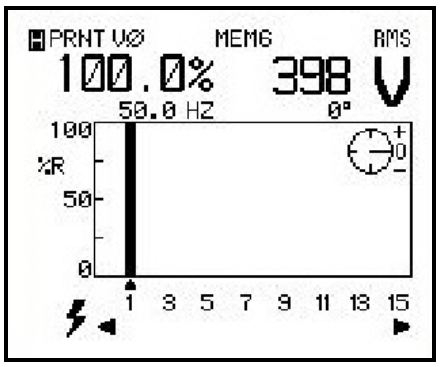

Fig. 14. Harmonics spectrum of the supply voltage.

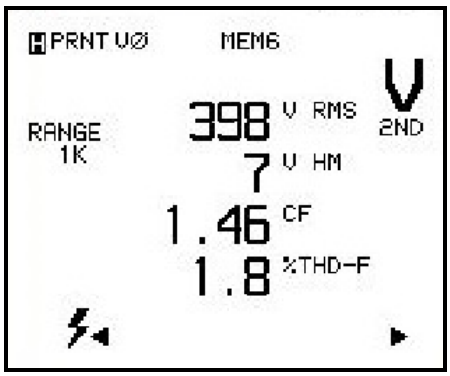

Fig. 15. The screen with the numerical values related to the supply voltage.

V. CONCLUSIONS

This paper described an application of the direct power control in a three-phase shunt active filtering system.

Both the modeling and experimental implementation of this specific control algorithm are relatively simple and effective at low currents.

In order to confirm the control strategy's great performance, numerous simulation are conducted, demonstrating how the non-sinusoidal load current can be changed to a quasi-sinusoidal current after the active filtering application.

Since the reactive power is zero after compensation and the active power closely follows its reference, an almost unity power factor is assured.

The simulation results are validated by the experimental results.

The experimental results were obtained within the Research Centre for Electrical Engineering of the University of Craiova, by using the dSPACE 1103 interface.

ACKNOWLEDGMENT

Source of research funding in this article: Research program of the Electrical Engineering Department financed by the University of Craiova.

Contribution of authors:
First author – 40%
First coauthor – 20%
Second coauthor – 20%
Third coauthor – 20%

Received on July 18, 2023
Editorial Approval on November 26, 2023

REFERENCES

[1] D. Li, T. Wang, W. Pan , X. Ding , and J. Gong, "A comprehensive review of improving power quality using active power filters," *Electric Power Systems Research*, 199, 2021, 107389.

[2] J. R. Rodriguez, J. W. Dixon, J. R. Espinoza, and J. Pontt, "PWM regenerative rectifiers: state of the art," *IEEE Trans. Ind. Electron.*, 2005, 52, (1), pp. 5–22.

[3] A. Kusko, M. T. Thompson, *Power Quality in Electrical Systems*, McGraw Hill Professional, 2007.

[4] T. Ohnishi, "Three-phase PWM converter/inverter by means of instantaneous active and reactive power control," *Proc. IEEE IECON'91*, Kobe, Japan, October/November 1991, pp. 819–824.

[5] H. Akagi, E..H. Watanabe, and M. Aredes, "Instantaneous power theory and applications to power conditioning," *IEEE Press Series on Power Engineering*, 2007, 1st edn.

[6] P. Noguchi, H. Tomiki, S. Kondo, and I Takahashi, "Direct power control of PWM converter without power-source voltage sensors," *IEEE Trans. Ind. Appl.*, 1998, 34, (3), pp. 473–479.

[7] B. S. Chen and G. JoÓs, "Direct power control of active filters with averaged switching frequency regulation," *IEEE Trans. Power Electron.*, vol. 23, no. 6, pp. 2729-2737, Nov. 2008.

[8] F. Tlili, F. Bacha, "Comparative study based on different switching lookup tables for Direct Power Control of three-phase AC/DC converter," *2020 4th International Conference on Advanced Systems and Emergent Technologies*, pp. 152-157.

[9] A. Chaoui, J. -P. Gaubert, F. Krim and L. Rambault, "Direct Power Control of shunt active filter," *2007 European Conference on Power Electronics and Applications*, Aalborg, Denmark, 2007, pp. 1-11.

[10] S. Chen and G. Joos, "Direct power control of three phase active filter with minimum energy storage components," *Proc. IEEE APEC'01*, Anaheim, USA, March 2001, pp. 570–576.

[11] T. A. Trivedi, R. Jadeja, P. Bhatt, "A review on Direct Power Control for applications to grid connected PWM converters," *Engineering, Technology & Applied Science Research*, vol. 5, no. 4, 2015.

[12] J. Alonso-Martinez,.G. Carrasco JE, and S. Arnaltes, "Table-based direct power control: a critical review for microgrid application," *IEEE Trans. Power Electron.*, 2010, 25, (12), pp. 2949–2961.

[13] A. Baktash, A. Vahedi, and M. A. S. Masoum "Improved switching table for direct power control of three-phase PWM rectifier," *Proc. Australasian Universities Power Engineering Conference*, Perth, Australia, December 2007, pp. 1–5.

[14] A. Bouafia, J. P. Gaubert, and F. Krim, "Analysis and design of new switching table for direct power control of three-phase PWM rectifier," *Proc. Power Electronics and Motion Control Conf.*, Poznan, Poland, September 2008, pp. 703–709.

[15] J. Hu, and Z. Q. Zhu, "Investigation on switching patterns of direct power control strategies for grid-connected dc-ac converters based on power variation rates," *IEEE Trans. Power Electron.*, 2011, 26, (12), pp. 3582–3598.

[16] B. Essoussi, A. Moutabir, B. Bensassi, A. Ouchatti, Y. Zahraoui, B. Benazza, "Power quality improvement using a new DPC switching table for a three-phase SAPF," *International Journal of Robotics and Control Systems*, vol. 3, no. 3, pp. 510-529, 2023.

[17] J. G. Norniella, J. M. Cano, and G. A. et al. Orcajo, "Optimization of direct power control of three-phase active rectifiers by using multiple switching tables," *Proc. Int. Conf. Renewable Energies and Power Quality (ICREPQ'10)*, Granada, Spain, March 2010.

[18] H. Jingjing, Z. Aimin, C. Xiaoju, Z. Hang, and W. Jianhua, "A novel direct power control strategy of double hysteresis and multiple switching tables for rectifiers," *Proc. Int. Conf. Advanced Power System Automation and Protection (APAP)*, Beijing, China, October 2011, pp. 36–41.

[19] A. Rath and G. Srungavarapu, "An advanced shunt active power filter (SAPF) for non-ideal grid using predictive DPC," *IETE Technical Review*, vol. 40, no. 4, pp. 1–14, Oct. 2022.

[20] Boudechiche, M. Sarra, O. Aissa, J.-P. Gaubert, B. Benlahbib, and A. Lashab, "Anti-windup FOPID-based DPC for SAPF interconnected to a PV System Tuned Using PSO Algorithm," *European Journal of Electrical Engineering*, vol. 22, no. 4-5, pp. 313–324, Oct. 2020.

[21] Z. Chelli, A. Lakehal, T. Khoualdia, and Y. Djeghader, "Study on Shunt Active Power Filter control strategies of three-phase grid-connected photovoltaic systems," *Periodica Polytechnica Electrical Engineering and Computer Science*, vol. 63, no. 3, pp. 213–226, Aug. 2019.

[22] M. Kadem, A. Semmah, P. Wira, and S. Dahmani, "Fuzzy logic-based instantaneous power ripple minimization for direct power control applied in a shunt active power filter," *Electrical Engineering*, vol. 102, no. 3, pp. 1327–1338, Sep. 2020.

[23] I. Takahashi and T. Noguchi, "A new quick-response and high-efficiency control strategy of an induction motor," *IEEE Trans. Ind. Appl.*, 1986, 22, (5), pp. 820–827.

[24] M. D. Constantinescu, M. Popescu, G. -E. Subtirelu and I. -C. Toma, "Application of the Direct Power Control in a three-phase shunt active power filter system," *2023 International Conference on Electromechanical and Energy Systems (SIELMEN)*, Craiova, Romania, 2023, pp. 1-6.